Liver Cancer 2014;3:71–84
DOI: 10.1159/000343863
Published online: May 8, 2014

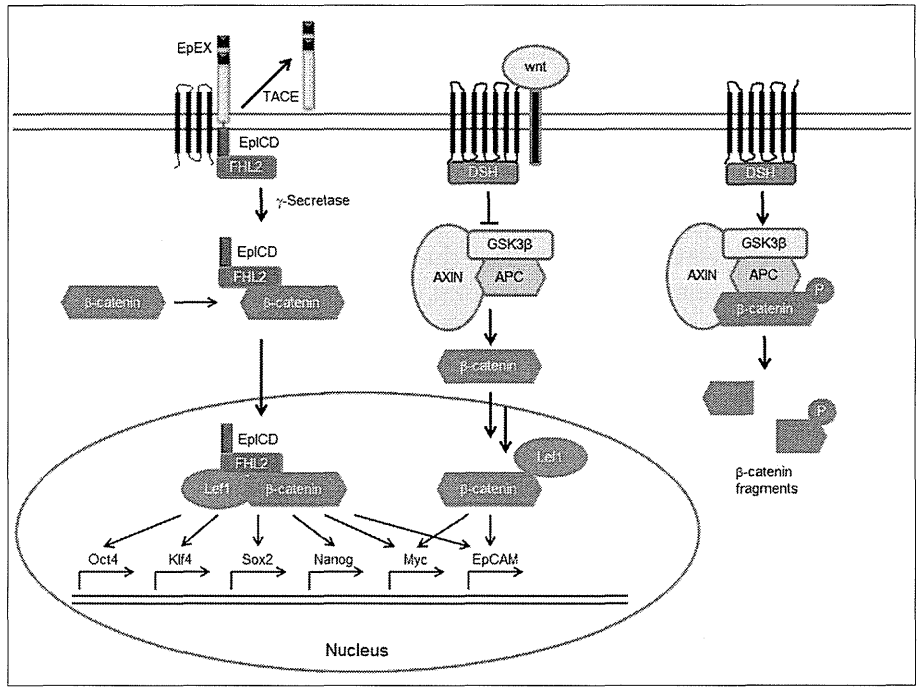

Color version available online

Fig. 1. Overview of cross-talk between EpCAM signaling and the Wnt pathway. Following cleavage by TACE/PS-2, EpICD translocates to the nucleus in a multiprotein complex. This nuclear complex binds the promoters of genes involved in cell cycle regulation and stemness. EpCAM regulates Nanog, Oct4, Klf4, Sox2, and Myc.

EpCAM Signaling Pathway

EpCAM is a type 1 transmembrane glycoprotein consisting of a large extracellular (EpEX), a single transmembrane and a short intracellular (EpICD) domain. Three independent glycosylation sites in the EpEX part dictate the stability of the whole protein at the cell surface. Liver CSC markers such as EpCAM, CD44, and CD133 share a number of entities and represent the most frequently used markers for the enrichment of tumor-initiating cells from primary human cancer. As is the case for many cell adhesion molecules, EpCAM has dual properties in that it can mediate cell-to-cell contact as well as transmit signals from the plasma membrane to the nucleus in order to regulate gene transcription [8]. In addition, EpCAM is not solely expressed in epithelial cells, but is also strongly expressed in various tissue stem cells, precursors, and in embryonic stem cells of murine and human origin [9]. Its mode of signaling proceeds via regulated intramembrane proteolysis and is activated by regulated intramembrane proteolysis (RIP) and the shedding of its EpEX [8] Sequential cleavage of EpCAM by tumor necrosis-factor alpha converting enzyme (TACE/ADAM17) and a gamma-secretase complex containing presenilin 2 (PS-2) results in the release of EpEX into the culture medium, and the release of the EpICD into the cytoplasm (fig. 1). EpICD then becomes part of a large nuclear complex containing transcriptional regulators β-catenin and Lef, which are both components of Wnt/β-catenin signaling. Four and one-half LIM domain protein 2 (FHL2) is essential for signal transduction by EpCAM, and FHL2 further regulates the localization and activity of TACE and PS-2. Through its function as a co-activator of β-catenin, FHL2 links EpICD with specific DNA sequences and gene regulation. FHL2 also has the potential to serve as a scaffolding protein for various signaling proteins used by EpCAM [10].

Wnt/β-CateninSignaling Pathway

The Wnt/β-catenin pathway is evolutionarily well-conserved and is essential for normal cellular processes such as development, growth, survival, regeneration, and self-renewal [11]. Disruption of Wnt/β-catenin signaling results from both genetic and epigenetic changes and is associated with a range of diseases including many cancers, especially colonic cancer and HCC. Disrupted Wnt/β-catenin signaling by mutational and non-mutational events is observed in around one third of all HCCs, emphasizing the importance of this pathway in hepatocarcinogenesis [12]. The Wnt pathway diversifies into two main branches, canonical (β-catenin-dependent) and non-canonical (β-catenin-independent), which play critical roles in specifying cellular fates and movements, respectively, during both embryonic development and adult tissue regeneration [13].

Wnt ligands signal through binding to seven transmembrane Frizzled (Fzd) receptors and single transmembrane lipoprotein receptor-related protein (LRP) 5 or 6 co-receptors. Canonical signaling mediated by ligands such as Wnt3a inhibits a multiprotein degradation complex consisting minimally of axin, adenomatous polyposis coli, and glycogen synthase kinase 3β. This inhibition culminates in the nuclear translocation of β-catenin, enabling it to interact with T-cell factor (TCF)/lymphoid enhancer factor (LEF) transcription factors to regulate gene expression. The resulting accumulation of β-catenin in the cytoplasm allows for its transfer into the nucleus, where it interacts with transcription factors of the LEF1 family. This functional complex induces the transcription of prominent targets like CD44 [14], cyclin D1 [15], and c-myc [16], which is also a major target of EpCAM signaling [17]. Moreover, c-myc can trigger the induction of a stem-like transcriptional profile in normal and cancer cells and represents the central switch from adult to embryonic stem cells [18].

Thus far, it remains unknown at which point in the signaling cascades of EpCAM and Wnt/Frizzled cross-talk occurs. However, EpICD does not only interact with β-catenin and Lef-1, it also binds to Lef-1 consensus sites in the promoter of Wnt target genes such as cyclin D1. EpICD appears to be essential for the formation of one of the two major nuclear protein/DNA complexes formed at Lef-1 consensus sites in EpCAM-positive carcinoma cells [10]. This suggests that EpICD can provide additional levels of regulation to Wnt target genes, which are central in cell cycle regulation, and thus could play important roles in self-renewal. Since Wnt signaling is reportedly instrumental in tumor-initiating cells (TICs), and because TICs rely on Wnt pathway-inducing signals from their microenvironment for the maintenance of their phenotype [19], it is tempting to speculate that EpCAM overexpression and signaling are also instrumental in this.

In addition to c-myc, other key factors such as Nanog, Klf4, Sox2, and Oct4, which are central to the conversion of somatic cells into induced pluripotent stem cells (iPS), have also been described as direct targets of EpCAM in human embryonic stem cells [20]. EpCAM possesses a crucial role in the induction and/or maintenance of the phenotype of tissue precursors, stem cells, iPS cells, and TICs. This function most likely relates primarily to the proliferation and the maintenance of an undifferentiated state. In the liver, EpCAM expression and Wnt signaling are both associated with a tissue stem cell phenotype and regenerative capacity of cells [21]. It is important to note that EpCAM expression is only detected in regenerating cells such as hepatobiliary stem cells and progenitor cells [21]. The interrelationship of EpCAM and Wnt in HCCs has been further substantiated upon by the finding that the EpCAM gene becomes transcriptionally activated by Tcf-4, a member of the Lef family of transcription factors. EpCAM is a marker for TICs with a stem/progenitor phenotype in HCC [22].

Non-canonical signaling, which is much less defined, is mediated by ligands such as Wnt11 that use the same Fzd receptors. The Wnt-Fzd-G protein complex can also stimulate p38 kinase and activate phosphodiesterase 6, which hydrolyzes cyclic GMP and results in the inactivation of protein kinase G and an increase in intracellular calcium. Wnt-mediated

increases in intracellular Ca^{2+} activate calcineurin and subsequently the nuclear factor of activated T-cells (NF-AT) family of calcineurin-dependent transcription factors, as well as TAK1-Nemo-like kinase (NLK) kinases. Signaling through the TAK-NLK kinases is proposed to inhibit canonical Wnt signaling, stimulating the Jun NH2-terminal kinase [23], calcium-calmodulin-dependent protein kinase II and protein kinase C pathways. These pathways interact with each other, and, in some cases, non-canonical signaling antagonizes the canonical pathway [24].

SALL4 Signaling Pathway

The human homologue of the Drosophilia spalt homeotic gene, SALL4, encodes a C2H2 zinc-finger transcription factor. It is one of the key factors for maintenance of pluripotency and self-renewal of embryonic stem cells, potentially through the interaction with Oct4, Sox2, and Nanog. SALL4 is known to encode two isoforms, namely SALL4A and SALL4B, and recent studies have suggested the important role of SALL4B on maintaining the stemness of embryonic stem cells [25]. In the liver, SALL4 is expressed at high levels in fetal-liver progenitor cells but not in adult hepatocytes, and it plays a critical role in hepatic cell lineage commitment. Recently, this oncofetal gene was identified as a marker of a subtype of HCC with progenitor-like features and is associated with a poor prognosis [26, 27].

SALL4 affects phosphatase and tensin homologue (PTEN) and phosphatidylinositol 3-kinase (PI3 K)-AKT signaling thorough the interaction with NuRD (nucleosome remodeling and histone deacetylase (HDAC)) complex. Since SALL4 is a known inhibitor of PTEN, the silencing of it reduces pAKT levels and blocks PI3 K survival signaling in HCC cells highly expressing SALL4. Furthermore, SALL4-positive HCC cells tend to show high HDAC activity and chemosensitivity to HDAC inhibitors such as suberic bis-hydroxamic acid and suberoylanilide hydroxamic acid. Consistently, HDAC inhibitors might be useful for the eradication of SALL4-positive HCC cells through their inhibitory effects on histone deacetylation of NuRD.

TGF-β Family

The TGF-β family plays a vital role in the control of proliferation and cellular differentiation in both stem cells and cancer cells. Impaired TGF-β signaling through the activation of interleukin-6 in hepatic stem/progenitor cells can contribute to altered differentiation patterns and HCC development [28]. TGF-β inhibits cell proliferation and promotes tumor cell invasion by inducing epithelial-mesenchymal transition (EMT). Reduced expression of the TGF-β receptor might be a key factor in shifting to the late response to TGF-β. Many studies have reported a reduction of TGF-β receptors in up to 70% of HCCs. Moreover, reduced TGF-β receptor 2 expression in HCC has been correlated with intrahepatic metastasis. TGF-β levels in the serum and urine are increased in HCC patients, while up to 40% of HCCs have increased TGF-β expression based on immunohistochemical analysis. In addition, high TGF-β levels have been correlated with advanced clinical stages of HCC. This dual role of TGF-β signaling in HCC is explained by its effect on the tumor tissue microenvironment and on the selective loss of the TGF-β-induced antiproliferative pathway. Tumor cells that have selectively lost their growth-inhibitory responsiveness to TGF-β, but retain an otherwise functional TGF-β signaling pathway may exhibit enhanced migration and invasive behavior in response to TGF-β stimulation. Recently, loss of the TGF-β adaptor and signaling molecule embryonic liver fodrin in the liver was found to cause cancer through deregulated hepatocyte proliferation and stimulation of angiogenesis. More recently, it was reported that HCC cells positive for signal transducers and activators of transcription-3/Oct4, have dysfunctional TGF-β signaling, and are likely cancer progenitor cells with the potential to give rise to HCC [29].

Other Pathways

The Notch signaling pathway plays an important role in stem cell self-renewal and differentiation.

However, other signaling pathways influence whether Notch functions as a tumor suppressor or oncogene depending on the particular tissue [30]. Notch signaling plays a well-defined role in liver embryogenesis and bile duct formation. In addition, Notch family members are involved in angiogenesis and endothelial sprouting. The increased expression of genes involved in this pathway has been shown in CD133-positive liver cancer cells compared to CD133-negative cells. The activated intracellular form of Notch-3, as well as the Notch ligand Jagged, is highly expressed in HCC. Conversely, Notch-1 has been reported to function as a tumor suppressor and participate in cross-talk with other signaling pathways such as Ras/Raf/Mitogen-activated protein kinase/ERK kinase (MEK)/extracellular-signal-regulated kinase (ERK) through the regulation of the PTEN tumor suppressor. Recent evidence indicates that activation of Notch-1 signaling increases the expression level of death receptor 5 (DR5) with enhancement of TNF-related apoptosis-inducing ligand induced apoptosis *in vitro* and in vivo [31].

Conserved from Drosophilia to humans, the Hedgehog (HH) pathway has a central role in embryonic development and adult tissue homeostasis by controlling cell fate specification and pattern formation [32]. The functional importance of this pathway is illustrated by the multiple birth defects and malignancies associated with mutations and/or aberrant activation of the pathway. Three HH ligands Sonic, Indian, and Desert have been identified in mammals that can bind interchangeably to two related twelve-pass membrane patched receptors. After ligand stimulation, Gli, like β-catenin, accumulates in the nucleus and induces transcription of genes related to the cell cycle and growth including insulin-like growth factor-2, cyclins, and β-catenin. Sonic is the predominant isoform in the liver. Up to 60% of human HCCs express Sonic, and the concomitant downregulation of Gli-related target genes is observed after the specific blockade of this pathway. Furthermore, tumorigenic activation of Smo can mediate overexpression of c-myc, a gene known to play an important pathogenic role in liver carcinogenesis. Recent studies have also shown that activation of Hedgehog signaling is critically related to CSCs and EMT features in many types of cancers including colonic, gastric, esophageal, hepatic, and others [33, 34].

microRNAs

Micro-ribonucleic acids (miRNAs) play critical roles in many biological processes including cancer by directly interacting with specific messenger RNAs (mRNAs) through base pairing, then inhibiting the expression of target genes through a variety of molecular mechanisms. MiRNAs can undergo aberrant regulation during carcinogenesis, and can act as oncogenes or tumor suppressor genes. Disruption of miRNA expression levels in tumor cells may result from distorted epigenetic regulation of miRNA expression, abnormalities in miRNA processing genes and proteins, and the location of miRNAs at cancer-associated genomic regions. Consequently, abnormal miRNA expression is a ubiquitous feature of solid tumors, including HCC. In liver carcinogenesis, miRNAs have been shown to have both tumor suppressive (miR-122, miR-26, miR-223) and oncogenic (miR-130b, miR-221, miR-222) activity [35–39]. Clearly, miRNAs play a critical role in carcinogenesis and oncogenesis. Emerging evidence suggests that certain abnormal miRNA expression levels cause cancer stem cell dysregulation, resulting in unlimited self-renewal and cancer progression. Therefore, miRNA expression is a vital key to CSC dysregulation. The let-7 miRNA precursor, which binds to the mRNA Lin28 (a marker of human embryonic stem cells), is regulated by the product of the oncogene c-myc. Let-7 family members are downregulated in malignancies, including HCC, and are associated with CSCs. The family members Lin28 and Lin28B

each target and inhibit let-7, and Lin28 and Lin28B are overexpressed in primary human tumors and human cancer cell lines, with an overall frequency of 15%. The mammalian homologs of Lin28 bind to the terminal loop of the precursors of let-7 family miRNAs and block their processing into mature miRNAs. Let-7 suppresses the expression of c-myc, which inhibits the transcription of let-7. Loss of such a negative feedback loop appears to be a common event in cancer cells from advanced-stage tumors such as HCC. MiR-181 regulates the Wnt/β-catenin signaling pathway in a positive feedback loop within stem cells. MiR-181 family members are highly expressed in embryogenic livers and isolated hepatic stem cells.

MiR-181 promotes the stem-cell-like features of HCC cells by targeting mRNAs that encode caudal type homeobox transcription factor 2 (CDX2) and GATA6, which are hepatic transcriptional regulators of differentiation. It also inhibits the mRNA that encodes NLK, an inhibitor of Wnt/β-catenin signaling, and maintains HCC stemness by inhibiting CDX2, GATA6, or NLK. Hepatic transcriptional regulators of differentiation and an inhibitor of Wnt/β-catenin signaling are directly targeted by miR-181. This type of positive feedback loop might be used by cancer cells to continuously self-propagate and contribute to metastasis and drug resistance.

Epigenetic Regulation of Hepatic Stem/Progenitor Cells

Although various genes have been identified as stem cell related, the control of stem cells is likely to arise from an integrated expression pattern of multiple genes involved in proliferation and differentiation rather than decimal gene expression [40]. In the self-renewal process of stem cells, it is important that the gene expression pattern is inherited in daughter cells after cell division. Therefore, chromatin regulation is a newly considered parameter that controls and integrates the expression of multiple genes. Chromatin modifying enzymes regulate the expression of target genes by manifesting structural changes in chromatin. As an epigenetic code, this forms the basis of stem cell identity and determines its responsiveness to extrinsic signals at successive developmental stages. In fact, progression from undifferentiated stem cells toward their differentiated progeny is characterized by alterations in the epigenetic landscapes of regulatory and coding regions of genes. The enzyme complex responsible for histone modification regulates activation and inactivation of transcription through methylation and acetylation of lysine residues in histone H3 and H4 [41]. In particular, histone modifications have been shown to affect polycomb group proteins such as Bmi1 and Ezh2 involved in stem cell regulation.

Recently, the bivalent domains, consisting of active modification H3K4me3 and repressive modification H3K27me3, have been shown to play an important role in the mechanism of action of histone modification proteins in stem cells [42]. Functional analyses of these molecules during liver development have advanced the understanding of several complex chromatin-modifying enzymes involved in cell lineage commitment [43]. In addition, it is reported that the expression of liver-specific transcription factors is changed by the administration of histone deacetylase inhibitors *in vitro* [44]. Special attention is being paid to their role in controlling both the growth and differentiation of stem cells *in vitro*.

Therapeutic Target of Molecular Signaling

The successful eradication of malignancy requires anticancer therapy that affects the differentiated neoplastic cells and the potential CSC population [45–47]. At present, conventional anticancer therapies include chemotherapy, radiation, and immunotherapy that kill

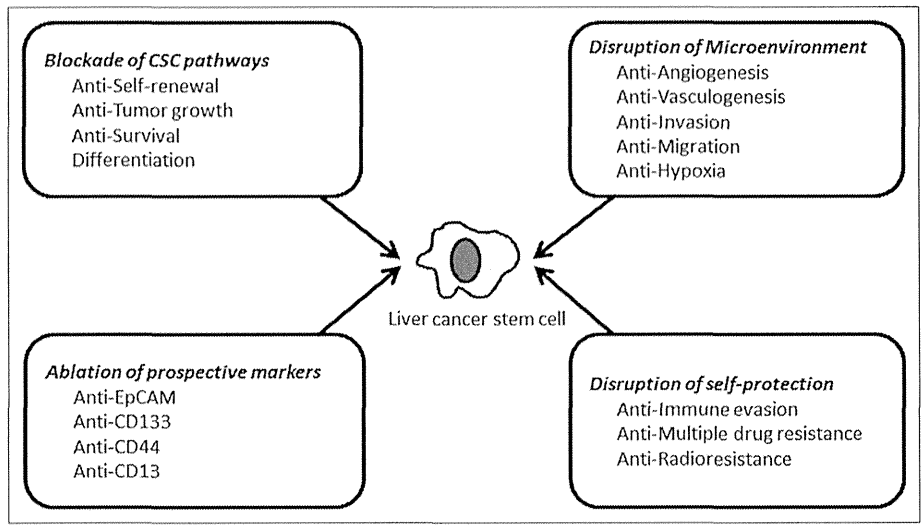

Fig. 2. Strategies to eradicate liver CSCs. CSCs are protected from conventional therapies by changing their microenvironment and self-protection. Specifically targeting any of these areas may lead to the eradication of CSCs.

rapidly growing differentiated tumor cells, thus reducing tumor mass, but potentially leaving behind cancer-initiating cells. Therapies that exclusively address the pool of differentiated cancer cells but fail to eradicate the CSC compartment might ultimately result in relapse and the proliferation of therapy-resistant and more aggressive tumor cells. An ideal drug regime would kill differentiated cancer cells and, at the same time, specifically, selectively, and rapidly target and kill CSCs to avoid toxic side effects in other cell types and to disrupt the self-protection potential of CSCs. CSCs clearly have a complex pathogenesis, with the potential for considerable crosstalk and redundancy in signaling pathways; hence, the targeting of single molecules or pathways may have a limited benefit. Combinations of therapies may be needed to overcome the complex network of signaling pathways, and ultimately inhibit the signaling that controls tumor growth and survival. In addition to the factors possessed by CSCs themselves, their microenvironment is also important for their maintenance, such as angiogenesis, vasculogenesis, and hypoxia. Many new therapeutic strategies targeting CSCs at various stages of differentiation or targeting the microenvironment have been attempted, as will be discussed below (fig. 2).

Liver Stem/Progenitor Cell Markers

The identification of CSC markers and their exploitation in targeted chemotherapy is an important research goal. It has been shown that CSCs in HCC can be identified on the basis of several cell surface antigens (CD133, CD90, CD44, OV6, and EpCAM), or the presence of side population (SP) cells with Hoechst dye-staining. Given the phenotypic similarities between CSCs and normal stem cells, it is reasonable to infer that the surface phenotype of CSCs resembles that of normal hepatic stem cells.

EpCAM as a Target in Cancer Therapy

EpCAM is potentially a promising target as it is highly expressed in most cancer cells as well as on CSCs. In normal tissue, EpCAM is arranged in a complex with CD9, CD44, and Claudin-7, and is localized to basolateral membranes. Thus, the accessibility for EpCAM-binding antibodies is lower in normal cells than for cancer cells. In cancer cells, EpCAM is strongly overexpressed and so it might be partly unbound and more accessible for targeting antibod-

ies. Several chimeric (chimeric Edrecolomab), humanised (3622W94), human-engineered (ING-1), and fully human (Adecatumumab) anti EpCAM antibodies with different target affinities have also been designed. Antibodies with the highest affinities such as 3622W94 and ING-1 induced acute pancreatitis even at low concentrations (1 mg/kg body weight) [48] because of increased binding of EpCAM-specific antibodies to healthy tissue such as pancreas and the respiratory tract. By contrast, the human antibody Adecatumumab (MT201), with an intermediate affinity, has shown only minor side effects such as nausea, chills, fatigue, and diarrhea, even at high doses (2–6 mg/kg body weight) [49]. In a clinical phase 2 trial, randomization between high and low EpCAM expression in metastatic breast cancer revealed that high EpCAM levels are associated with a good prognosis in terms of overall survival after treatment with Adecatumumab. In 2009, the first antibody targeting EpCAM, Catumaxomab (Removab), obtained approval for the European market. This trifunctional antibody has the ability to bind EpCAM-expressing cancer cells as well as cytotoxic T-cells via the CD3 receptor. Clinical trials revealed humoral responses against this antibody after treatment, which might be due to the chimeric structure consisting of mouse IgG2a and rat IgG2b. The type of response against Catumaxomab correlated positively with the clinical outcome, and its use in patients with malignant ascites prolonged their overall survival [50]. Recently, the bispecific antibody MT110 was tested for its ability to target TICs derived from colorectal cancers. This antibody has binding affinities for EpCAM and CD3, which allows it to initiate the formation of a cytolytic synapse between T-cells and TICs. A combination of this antibody and peripheral blood mononuclear cells led to decreased or absent colony formation in soft agar assays. Moreover, treatment with MT110 prevented tumor formation in a xenograft model where mice were inoculated with TICs [51].

Based on the novel understanding of the functions of EpCAM, another interesting approach relies on the interface with the EpCAM signaling cascade. The knowledge of proteases involved in the activating proteolytic cleavage of EpCAM allows for the systematic testing of combinations of protease inhibitors. The inhibition of the EpICD-FHL2 interaction by small molecules generated from structure based rational design and bioinformatics is a promising and highly innovative strategy to specifically target EpCAM and its signaling. In liver cells, RNA interference targeting of EpCAM significantly decreased the CSC pool and reduced both the tumorigenicity and invasive capacity of CSCs. Since EpCAM expression is a downstream target of Wnt/β-catenin, these results may have implications for the development of novel target therapies.

Blockage of CSC Pathways

Anti-Self-Renewal

The targeting of key signaling pathways for CSC self-renewal is another approach to therapy. The Wnt/β-catenin signaling pathway is important for the self-renewal and maintenance of stem cells [52], and several studies have demonstrated decreased proliferation and increased apoptosis following its inhibition [53]. The pathway can be inhibited in a number of ways; for example, Dickkopf1 (Dkk1) binds to the low density lipoprotein receptor-related protein-6 (LRP6) and prevents the formation of the Frizzled-Wnt-LRP6 complex [54]. A new approach to antagonize Wnt signaling has been the development of small molecules (XAV939) to inhibit the enzyme tankyrase that normally destroys the scaffold protein axin, a crucial component of the β-catenin destruction complex [55]. Furthermore, many antibody-based therapeutic approaches targeting EpCAM are currently being developed that will be efficacious in eradicating EpCAM-expressing cancer stem cells.

The Hedgehog pathway is another potential target for CSC eradication. Several small-molecule modulators of Sonic hedgehog signaling have been used to regulate the activity of this pathway in medulloblastoma, basal cell carcinoma, pancreatic cancer, prostate cancer,

and developmental disorders [56]. In liver cells, the suppression of the Sonic Hedgehog pathway by small interfering RNA not only decreased HCC cell proliferation but also chemosensitized the cells to 5-fluorouracil (5-FU) and to the induction of cell apoptosis [57]. Furthermore, in hepatoblastoma, blocking Hh signaling with the antagonist cyclopamine had a strong inhibitory effect on cell proliferation of HB cell lines [58]. Overall, it is likely that the targeting of intracellular pathways associated with self-renewal of CSC will become established in the near future.

Differentiation

CSCs, which make up only a small proportion of cancer cells, have the capacity to sustain tumor growth and are more resistant to conventional chemotherapy than other more differentiated cancer cells. One approach to treat malignancies, therefore, is to induce their differentiation. Differentiation therapy could force hepatoma cells to differentiate and lose their self-renewal property. Hepatocyte nuclear factor-4α, a central regulator of the differentiated hepatocyte phenotype, suppresses tumorigenesis and tumor development by inducing the differentiation of hepatoma cells, especially CSCs [59]. Interferon therapy is effective not only for eradicating hepatitis viruses, but also for preventing the development of HCC regardless of the virological response. Interferon alpha treatment accelerates hepatocytic and biliary differentiation in oval cell lines [60], and could be used to treat HCC by targeting CSCs. In addition, oncostatin M (OSM), an interleukin-6 related cytokine known to induce the differentiation of hepatoblasts into hepatocytes, could be used to effectively induce the differentiation and active cell division of dormant EpCAM-positive liver CSCs. Moreover, a combination of OSM and conventional chemotherapy with 5-FU efficiently eliminates HCC by targeting both CSCs and non-CSCs [61]. These findings indicate that differentiation therapy combined with conventional chemotherapy may be an effective treatment of HCC.

Future Directions

The rapid development of the CSC field combined with genome-wide screening techniques has enabled the identification of important new CSC markers and pathways, which have contributed to one of the most important developments in cancer treatment. However, several important issues remain to be resolved, and little is known about CSC-directed therapies (e.g., targeting EpCAM in EpCAM-positive liver CSCs). Initial results are promising, but knowledge of the potential short- and long-term side effects of these therapies is limited. For example, if not sufficiently specific for CSCs, such therapies could lead to tissue and/or organ damage from the depletion of reserve/regenerative stem cells. This could cause acute and irreversible organ failure.

New drug discoveries for CSCs are currently underway that aim to completely eradicate cancer. Recent studies have highlighted the importance and necessity of exploring the susceptibility of CSCs to existing therapies in combination with the disruption of key pathways controlling self-renewal, pluripotency, chemoresistance, radioresistance, and angiogenesis through molecular targeted therapy.

Other novel and important directions for effective therapies include the disruption of the tumor niche that is essential for CSC homeostasis, and the depletion of CSCs by forced differentiation. However, more work is required to advance our knowledge on the role of CSCs in tumor hierarchy and to design more effective and specific anti-CSC therapy. The current state of knowledge strongly indicates the advantage of targeting CSCs to improve the limited efficiency of existing therapies, and it has provided an important framework for the develop-

ment of novel therapeutic regimens with the ultimate hope of long-term clinical benefits to the patients.

Acknowledgements

This study was supported by a Grant-in-Aid from the Ministry of Education, Culture, Sports, Science and Technology, a grant from the Ministry of Health, Labour and Welfare, and a grant from the National Cancer Center Research and Development Fund (23-B-5), Japan.

References

1 el-Serag HB: Epidemiology of hepatocellular carcinoma. Clin Liver Dis 2001;5:87–107, vi vi.
2 Russo FP, Parola M: Stem and progenitor cells in liver regeneration and repair. Cytotherapy 2011;13:135–144.
3 Michalopoulos GK: Liver regeneration. J Cell Physiol 2007;213:286–300.
4 Yamashita T, Honda M, Nakamoto Y, Baba M, Nio K, Hara Y, Zeng SS, Hayashi T, Kondo M, Takatori H, Yamashita T, Mizukoshi E, Ikeda H, Zen Y, Takamura H, Wang XW, Kaneko S: Discrete nature of EpCAM+ and CD90+ cancer stem cells in human hepatocellular carcinoma. Hepatology 2013;57:1484–1497.
5 Kitisin K, Shetty K, Mishra L, Johnson LB: Hepatocellular stem cells. Cancer Biomark 2007;3:251–262.
6 Alison MR: Liver stem cells: implications for hepatocarcinogenesis. Stem Cell Rev 2005;1:253–260.
7 Katoh M: WNT signaling pathway and stem cell signaling network. Clin Cancer Res 2007;13:4042–4045.
8 Munz M, Baeuerle PA, Gires O: The emerging role of EpCAM in cancer and stem cell signaling. Cancer Res 2009;69:5627–5629.
9 Trzpis M, McLaughlin PM, de Leij LM, Harmsen MC: Epithelial cell adhesion molecule: more than a carcinoma marker and adhesion molecule. Am J Pathol 2007;171:386–395.
10 Maetzel D, Denzel S, Mack B, Canis M, Went P, Benk M, Kieu C, Papior P, Baeuerle PA, Munz M, Gires O: Nuclear signalling by tumour-associated antigen EpCAM. Nat Cell Biol 2009;11:162–171.
11 Branda M, Wands JR: Signal transduction cascades and hepatitis B and C related hepatocellular carcinoma. Hepatology 2006;43:891–902.
12 Ishizaki Y, Ikeda S, Fujimori M, Shimizu Y, Kurihara T, Itamoto T, Kikuchi A, Okajima M, Asahara T: Immunohistochemical analysis and mutational analyses of beta-catenin, Axin family and APC genes in hepatocellular carcinomas. Int J Oncol 2004;24:1077–1083.
13 Reya T, Clevers H: Wnt signalling in stem cells and cancer. Nature 2005;434:843–850.
14 Wielenga VJ, Smits R, Korinek V, Smit L, Kielman M, Fodde R, Clevers H, Pals ST: Expression of CD44 in Apc and Tcf mutant mice implies regulation by the WNT pathway. Am J Pathol 1999;154:515–523.
15 Tetsu O, McCormick F: Beta-catenin regulates expression of cyclin D1 in colon carcinoma cells. Nature 1999;398:422–426.
16 He TC, Sparks AB, Rago C, Hermeking H, Zawel L, da Costa LT, Morin PJ, Vogelstein B, Kinzler KW: Identification of c-MYC as a target of the APC pathway. Science 1998;281:1509–1512.
17 Münz M, Kieu C, Mack B, Schmitt B, Zeidler R, Gires O: The carcinoma-associated antigen EpCAM upregulates c-myc and induces cell proliferation. Oncogene 2004;23:5748–5758.
18 Wong DJ, Liu H, Ridky TW, Cassarino D, Segal E, Chang HY: Module map of stem cell genes guides creation of epithelial cancer stem cells. Cell Stem Cell 2008;2:333–344.
19 Malanchi I, Huelsken J: Cancer stem cells: never Wnt away from the niche. Curr Opin Oncol 2009;21:41–46.
20 Lu TY, Lu RM, Liao MY, Yu J, Chung CH, Kao CF, Wu HC: Epithelial cell adhesion molecule regulation is associated with the maintenance of the undifferentiated phenotype of human embryonic stem cells. J Biol Chem 2010;285:8719–8732.
21 de Boer CJ, van Krieken JH, Janssen-van Rhijn CM, Litvinov SV: Expression of Ep-CAM in normal, regenerating, metaplastic, and neoplastic liver. J Pathol 1999;188:201–206.
22 Yamashita T, Ji J, Budhu A, Forgues M, Yang W, Wang HY, Jia H, Ye Q, Qin LX, Wauthier E, Reid LM, Minato H, Honda M, Kaneko S, Tang ZY, Wang XW: EpCAM-positive hepatocellular carcinoma cells are tumor-initiating cells with stem/progenitor cell features. Gastroenterology 2009;136:1012–1024.
23 Weston CR, Davis RJ: The JNK signal transduction pathway. Curr Opin Genet Dev 2001;12:14–21.
24 Kühl M: Non-canonical Wnt signaling in Xenopus: regulation of axis formation and gastrulation. Semin Cell Dev Biol 2002;13:243–249.
25 Yuri S, Fujimura S, Nimura K, Takeda N, Toyooka Y, Fujimura Y, Aburatani H, Ura K, Koseki H, Niwa H, Nishinakamura R: Sall4 is essential for stabilization, but not for pluripotency, of embryonic stem cells by repressing aberrant trophectoderm gene expression. Stem Cells 2009;27:796–805.
26 Yong KJ, Chai L, Tenen DG: Oncofetal gene SALL4 in aggressive hepatocellular carcinoma. N Engl J Med 2013;369:1171–1172.

27 Zeng SS, Yamashita T, Kondo M, Nio K, Hayashi T, Hara Y, Nomura Y, Yoshida M, Hayashi T, Oishi N, Ikeda H, Honda M, Kaneko S: The transcription factor SALL4 regulates stemness of EpCAM-positive hepatocellular carcinoma. J Hepatol 2014;60:127–134.
28 Tang Y, Kitisin K, Jogunoori W, Li C, Deng CX, Mueller SC, Ressom HW, Rashid A, He AR, Mendelson JS, Jessup JM, Shetty K, Zasloff M, Mishra B, Reddy EP, Johnson L, Mishra L: Progenitor/stem cells give rise to liver cancer due to aberrant TGF-beta and IL-6 signaling. Proc Natl Acad Sci USA 2008;105:2445–2450.
29 Yuan F, Zhou W, Zou C, Zhang Z, Hu H, Dai Z, Zhang Y: Expression of Oct4 in HCC and modulation to wnt/β-catenin and TGF-β signal pathways. Mol Cell Biochem 2010;343:155–162.
30 Weng AP, Aster JC: Multiple niches for Notch in cancer: context is everything. Curr Opin Genet Dev 2004;14:48–54.
31 Androutsellis-Theotokis A, Leker RR, Soldner F, Hoeppner DJ, Ravin R, Poser SW, Rueger MA, Bae SK, Kittappa R, McKay RD: Notch signalling regulates stem cell numbers in vitro and in vivo. Nature 2006;442:823–826.
32 Cerdan C, Bhatia M: Novel roles for Notch, Wnt and Hedgehog in hematopoesis derived from human pluripotent stem cells. Int J Dev Biol 2010;54:955–963.
33 Villavicencio EH, Walterhouse DO, Iannaccone PM: The sonic hedgehog-patched-gli pathway in human development and disease. Am J Hum Genet 2000;67:1047–1054.
34 Lum L, Beachy PA: The Hedgehog response network: sensors, switches, and routers. Science 2004;304:1755–1759.
35 Coulouarn C, Factor VM, Andersen JB, Durkin ME, Thorgeirsson SS: Loss of miR-122 expression in liver cancer correlates with suppression of the hepatic phenotype and gain of metastatic properties. Oncogene 2009;28:3526–3536.
36 Pineau P, Volinia S, McJunkin K, Marchio A, Battiston C, Terris B, Mazzaferro V, Lowe SW, Croce CM, Dejean A: miR-221 overexpression contributes to liver tumorigenesis. Proc Natl Acad Sci USA 2010;107:264–269.
37 Ma S, Tang KH, Chan YP, Lee TK, Kwan PS, Castilho A, Ng I, Man K, Wong N, To KF, et al: miR-130b Promotes CD133(+) liver tumor-initiating cell growth and self-renewal via tumor protein 53-induced nuclear protein 1. Cell Stem Cell 2010;7:694–707.
38 Wong QW, Lung RW, Law PT, Lai PB, Chan KY, To KF, Wong N: MicroRNA-223 is commonly repressed in hepatocellular carcinoma and potentiates expression of Stathmin1. Gastroenterology 2008;135:257–269.
39 Wong QW, Ching AK, Chan AW, Choy KW, To KF, Lai PB, Wong N: MiR-222 overexpression confers cell migratory advantages in hepatocellular carcinoma through enhancing AKT signaling. Clin Cancer Res 2010;16:867–875.
40 Koike H, Taniguchi H: Characteristics of hepatic stem/progenitor cells in the fetal and adult liver. J Hepatobiliary Pancreat Sci 2012;19:587–593.
41 Strahl BD, Allis CD: The language of covalent histone modifications. Nature 2000;403:41–45.
42 Stock JK, Giadrossi S, Casanova M, Brookes E, Vidal M, Koseki H, Brockdorff N, Fisher AG, Pombo A: Ring1-mediated ubiquitination of H2A restrains poised RNA polymerase II at bivalent genes in mouse ES cells. Nat Cell Biol 2007;9:1428–1435.
43 Xu CR, Cole PA, Meyers DJ, Kormish J, Dent S, Zaret KS: Chromatin "prepattern" and histone modifiers in a fate choice for liver and pancreas. Science 2011;332:963–966.
44 Kubicek S, Gilbert JC, Fomina-Yadlin D, Gitlin AD, Yuan Y, Wagner FF, Holson EB, Luo T, Lewis TA, Taylor B, Gupta S, Shamji AF, Wagner BK, Clemons PA, Schreiber SL: Chromatin-targeting small molecules cause class-specific transcriptional changes in pancreatic endocrine cells. Proc Natl Acad Sci USA 2012;109:5364–5369.
45 Klonisch T, Wiechec E, Hombach-Klonisch S, Ande SR, Wesselborg S, Schulze-Osthoff K, Los M: Cancer stem cell markers in common cancers - therapeutic implications. Trends Mol Med 2008;14:450–460.
46 Dingli D, Michor F: Successful therapy must eradicate cancer stem cells. Stem Cells 2006;24:2603–2610.
47 Oishi N, Wang XW: Novel therapeutic strategies for targeting liver cancer stem cells. Int J Biol Sci 2011;7:517–535.
48 Goel S, Bauer RJ, Desai K, Bulgaru A, Iqbal T, Strachan BK, Kim G, Kaubisch A, Vanhove GF, Goldberg G, Mani S: Pharmacokinetic and safety study of subcutaneously administered weekly ING-1, a human engineere monoclonal antibody targeting human EpCAM, in patients with advanced solid tumors. Ann Oncol 2007;18:1704–1707.
49 Schmidt M, Scheulen ME, Dittrich C, Obrist P, Marschner N, Dirix L, Schmidt M, Rüttinger D, Schuler M, Reinhardt C, Awada A: An open-label, randomized phase II study of adecatumumab, a fully human anti-EpCAM antibody, as monotherapy in patients with metastatic breast cancer. Ann Oncol 2010;21:275–282.
50 Ott MG, Marmé F, Moldenhauer G, Lindhofer H, Hennig M, Spannagl R, Essing MM, Linke R, Seimetz D: Humoral response to catumaxomab correlates with clinical outcome: results of the pivotal phase II/III study in patients with malignant ascites. Int J Cancer 2012;130:2195–2203.
51 Herrmann I, Baeuerle PA, Friedrich M, Murr A, Filusch S, Rüttinger D, Majdoub MW, Sharma S, Kufer P, Raum T, Münz M: Highly efficient elimination of colorectal tumor-initiating cells by an EpCAM/CD3-bispecific antibody engaging human T cells. PLoS ONE 2010;5:e13474.
52 Yamashita T, Budhu A, Forgues M, Wang XW: Activation of hepatic stem cell marker EpCAM by Wnt-beta-catenin signaling in hepatocellular carcinoma. Cancer Res 2007;67:10831–10839.
53 Zeng G, Apte U, Cieply B, Singh S, Monga SP: siRNA-mediated beta-catenin knockdown in human hepatoma cells results in decreased growth and survival. Neoplasia 2007;9:951–959.
54 Li Y, Lu W, King TD, Liu CC, Bijur GN, Bu G: Dkk1 stabilizes Wnt co-receptor LRP6: implication for Wnt ligand-induced LRP6 down-regulation. PLoS ONE 2010;5:e11014.

55 Huang SM, Mishina YM, Liu S, Cheung A, Stegmeier F, Michaud GA, Charlat O, Wiellette E, Zhang Y, Wiessner S, Hild M, Shi X, Wilson CJ, Mickanin C, Myer V, Fazal A, Tomlinson R, Serluca F, Shao W, Cheng H, Shultz M, Rau C, Schirle M, Schlegl J, Ghidelli S, Fawell S, Lu C, Curtis D, Kirschner MW, Lengauer C, Finan PM, Tallarico JA, Bouwmeester T, Porter JA, Bauer A, Cong F: Tankyrase inhibition stabilizes axin and antagonizes Wnt signalling. Nature 2009;461:614–620.
56 Stanton BZ, Peng LF: Small-molecule modulators of the Sonic Hedgehog signaling pathway. Mol Biosyst 2010;6:44–54.
57 Wang Q, Huang S, Yang L, Zhao L, Yin Y, Liu Z, Chen Z, Zhang H: Down-regulation of Sonic hedgehog signaling pathway activity is involved in 5-fluorouracil-induced apoptosis and motility inhibition in Hep3B cells. Acta Biochim Biophys Sin (Shanghai) 2008;40:819–829.
58 Eichenmüller M, Gruner I, Hagl B, Häberle B, Müller-Höcker J, von Schweinitz D, Kappler R: Blocking the hedgehog pathway inhibits hepatoblastoma growth. Hepatology 2009;49:482–490.
59 Yin C, Lin Y, Zhang X, Chen YX, Zeng X, Yue HY, Hou JL, Deng X, Zhang JP, Han ZG, Xie WF: Differentiation therapy of hepatocellular carcinoma in mice with recombinant adenovirus carrying hepatocyte nuclear factor-4alpha gene. Hepatology 2008;48:1528–1539.
60 Lim R, Knight B, Patel K, McHutchison JG, Yeoh GC, Olynyk JK: Antiproliferative effects of interferon alpha on hepatic progenitor cells in vitro and in vivo. Hepatology 2006;43:1074–1083.
61 Yamashita T, Honda M, Nio K, Nakamoto Y, Yamashita T, Takamura H, Tani T, Zen Y, Kaneko S: Oncostatin m renders epithelial cell adhesion molecule-positive liver cancer stem cells sensitive to 5-Fluorouracil by inducing hepatocytic differentiation. Cancer Res 2010;70:4687–4697.

Fei Lan,[1] Hirofumi Misu,[1] Keita Chikamoto,[1,2] Hiroaki Takayama,[1] Akihiro Kikuchi,[1] Kensuke Mohri,[1] Noboru Takata,[1] Hiroto Hayashi,[1] Naoto Matsuzawa-Nagata,[1] Yumie Takeshita,[1] Hiroyo Noda,[1] Yukako Matsumoto,[1] Tsuguhito Ota,[1] Toru Nagano,[3] Masatoshi Nakagen,[3] Ken-ichi Miyamoto,[4,5] Kanako Takatsuki,[6] Toru Seo,[6] Kaito Iwayama,[7] Kunpei Tokuyama,[7] Seiichi Matsugo,[8,9] Hong Tang,[10] Yoshiro Saito,[11] Satoshi Yamagoe,[12] Shuichi Kaneko,[1] and Toshinari Takamura[1]

LECT2 Functions as a Hepatokine That Links Obesity to Skeletal Muscle Insulin Resistance

Diabetes 2014;63:1649–1664 | DOI: 10.2337/db13-0728

Recent articles have reported an association between fatty liver disease and systemic insulin resistance in humans, but the causal relationship remains unclear. The liver may contribute to muscle insulin resistance by releasing secretory proteins called hepatokines. Here we demonstrate that leukocyte cell–derived chemotaxin 2 (LECT2), an energy-sensing hepatokine, is a link between obesity and skeletal muscle insulin resistance. Circulating LECT2 positively correlated with the severity of both obesity and insulin resistance in humans. *LECT2* expression was negatively regulated by starvation-sensing kinase adenosine monophosphate–activated protein kinase in H4IIEC hepatocytes. Genetic deletion of *LECT2* in mice increased insulin sensitivity in the skeletal muscle. Treatment with recombinant LECT2 protein impaired insulin signaling via phosphorylation of Jun NH_2-terminal kinase in C2C12 myocytes. These results demonstrate the involvement of LECT2 in glucose metabolism and suggest that LECT2 may be a therapeutic target for obesity-associated insulin resistance.

Insulin resistance is a characteristic feature of people with type 2 diabetes (1) and plays a major role in the development of various diseases such as cardiovascular diseases (2) and nonalcoholic steatohepatitis (3,4). In an insulin-resistant state, impaired insulin action promotes hepatic glucose production and reduces glucose uptake by peripheral tissues. Insulin resistance is commonly observed in obese and overweight people, suggesting a potential role of ectopic fat accumulation in insulin-target tissues in mediating insulin resistance (5). However, the molecular mechanisms underlying insulin resistance are now known to be influenced by the abnormal secretion of tissue-derived factors such as adipokines (6–9), myokines (10,11), and hepatokines (12–14), which traditionally have been considered separate from the endocrine system.

Leukocyte cell–derived chemotaxin 2 (LECT2) is a secretory protein originally identified in the process of screening for a novel neutrophil chemotactic protein (15). LECT2 (encoded by the *Lect2* gene in humans) is expressed preferentially by human adult and fetal liver cells and is

[1]Department of Disease Control and Homeostasis, Kanazawa University Graduate School of Medical Sciences, Kanazawa, Ishikawa, Japan
[2]Division of Natural System, Graduate School of Natural Science and Technology, Kanazawa University, Kanazawa, Ishikawa, Japan
[3]Public Central Hospital of Matto Ishikawa, Hakusan, Ishikawa, Japan
[4]Department of Hospital Pharmacy, Kanazawa University Graduate School of Medical Sciences, Kanazawa, Ishikawa, Japan
[5]Department of Medicinal Informatics, Kanazawa University Graduate School of Medical Sciences, Kanazawa, Ishikawa, Japan
[6]Merck & Co. Inc., Rahway, NJ
[7]Division of Sports Medicine, Graduate School of Comprehensive Human Sciences, University of Tsukuba, Ibaraki, Japan
[8]Division of Material Engineering, Graduate School of Natural Science and Technology, Kanazawa University, Kanazawa, Japan
[9]Institute of Science and Engineering, Faculty of Natural System, Kanazawa University, Kanazawa, Japan
[10]Center of Infectious Diseases, West China Hospital of Sichuan University, Chengdu, China
[11]Department of Medical Life Systems, Faculty of Medical and Life Sciences, Doshisha University, Kyotanabe, Kyoto, Japan
[12]Department of Bioactive Molecules, National Institute of Infectious Diseases, Shinjuku-ku, Tokyo, Japan

Corresponding author: Toshinari Takamura, ttakamura@m-kanazawa.jp.

Received 6 May 2013 and accepted 14 January 2014.

This article contains Supplementary Data online at http://diabetes.diabetesjournals.org/lookup/suppl/doi:10.2337/db13-0728/-/DC1.

F.L. and H.M. contributed equally to this study.

secreted into the bloodstream (16). The early study using *Lect2*-deficient mice showed that LECT2 negatively regulates the homeostasis of natural killer T cells in the liver (17). Anson et al. (18) more recently reported that LECT2 exerts anti-inflammatory and tumor-suppressive actions in β-catenin–induced liver tumorigenesis. To date, however, the role of LECT2 in the development of obesity and insulin resistance induced by overnutrition has not yet been established.

We previously demonstrated that overproduction of the liver-derived secretory protein selenoprotein P (SeP) contributes to hyperglycemia in type 2 diabetes by inducing insulin resistance in the liver and skeletal muscle (12). SeP has emerged from comprehensive liver screenings for secretory proteins whose expression levels are correlated with the severity of insulin resistance in patients with type 2 diabetes (12,19,20). Based on these findings, we have proposed that, analogous to adipose tissue, the liver may participate in the pathology of type 2 diabetes and insulin resistance through the production of secretory proteins called hepatokines (12). Other liver-secreted proteins such as fetuin-A (21), angiopoietin-related protein 6 (22), fibroblast growth factor 21 (23), insulin-like growth factors (24), and sex hormone-binding globulin (25) have recently been reported as hepatokines that are involved in glucose metabolism and insulin sensitivity. However, the identification of hepatokines involved in fat accumulation was not adequate. In this study, we identified LECT2 as a hepatokine whose expression levels were positively correlated with the severity of obesity in humans. Levels of LECT2 in blood also were elevated in animal models with obesity. *Lect2*-deficient mice showed an increase of insulin signaling in skeletal muscle. Conversely, treatment with recombinant LECT2 protein impaired insulin signaling in C2C12 myotubes. Our data demonstrate that LECT2 functions as a hepatokine that links obesity to insulin resistance in skeletal muscle.

RESEARCH DESIGN AND METHODS

Human Clinical Studies

Liver samples to be analyzed by serial analysis of gene expression were obtained from five patients with type 2 diabetes and five nondiabetic subjects who underwent surgical procedures for malignant tumors, including gastric cancer, gall bladder cancer, and colon cancer. Liver samples to be subjected to DNA chip analysis were obtained from 22 patients with type 2 diabetes and 11 subjects with normal glucose tolerance using ultrasonography-guided biopsy needles. Detailed clinical information about these subjects is presented elsewhere (12,19).

Serum samples were obtained from 200 participants who went to the Public Central Hospital of Matto, Ishikawa, Japan, for a complete physical examination. Following an overnight fast, venous blood samples were taken from each patient. Serum levels of LECT2 were measured by an Ab-Match ASSEMBLY Human LECT2 kit (MBL Co.) (26,27).

The homeostasis model assessment of insulin resistance (HOMA-IR) was calculated using the following formula: HOMA-IR = [fasting insulin (μU/mL) × fasting plasma glucose (mmol/L)]/22.5 (28). All patients provided written informed consent for participation in this study. All experimental protocols were approved by the relevant ethics committees at our institution and Matto Ishikawa Central Hospital and were conducted in accordance with the Declaration of Helsinki.

Animals

Eight-week-old C57BL/6J mice were obtained from Sankyo Laboratory Service (Tokyo, Japan). All animals were housed in a 12-h light/12-h dark cycle and allowed free access to food and water. A 60% high-fat diet (HFD; D12492) was purchased from Research Diets (New Brunswick, NJ).

Purification of LECT2

Murine LECT2 was expressed and purified as previously described (29), with minor modifications. Briefly, LECT2 was stably expressed in CHO cells. The protein was purified from the cultured medium by ion exchange chromatography. The fractions containing LECT2 were subsequently applied to a mono S column (GE Healthcare) equilibrated with 50 mmol/L sodium phosphate buffer (pH 7.5) and eluted with a linear gradient of 150–350 mmol/L sodium chloride (NaCl).

Lect2 Knockout Mice

Lect2 knockout mice were produced by homologous recombination using genomic DNA cloned from an Sv-129 P1 library, as described previously (17). All experimental mice were generated from intercross between heterozygous mice, and littermates were divided into groups. Because female *Lect2* knockout mice had inconsistent phenotypes, only male mice were used in all experiments except those of starvation.

Materials

H4IIEC and C2C12 cells were purchased from the American Type Culture Collection (Manassas, VA). Human recombinant insulin was purchased from Sigma Aldrich (St. Louis, MO). Rabbit antiphospho-Akt (Ser473) monoclonal antibody, rabbit anti–total Akt polyclonal antibody, rabbit antiphospho-AMP-activated protein kinase (AMPK) (Thr172) monoclonal antibody, rabbit anti-AMPKα antibody, rabbit antiphospho-Jun NH_2-terminal kinase (JNK) (Thr183/Try185), rabbit anti-JNK, rabbit anti–binding immunoglobulin protein antibody, rabbit antiphospho-eIF2α (Ser51) antibody, rabbit anti–nuclear factor-κB p65 antibody, rabbit antiphospho-IκB kinase-αβ (Ser176/180) antibody, rabbit anti-IκB kinase-α antibody, and rabbit antiphospho-IκBα(Ser32) antibody were purchased from Cell Signaling Technology (Danvers, MA). Rabbit antileukocyte cell–derived chemotaxin 2 polyclonal antibody (sc-99036) and rabbit anti–glyceraldehyde-3-phosphate dehydrogenase polyclonal antibody were purchased from Santa Cruz Biotechnology (Santa Cruz, CA).

Transient Transfection Experiment

C2C12 myoblasts were grown in 12-well multiplates. When 30–50% confluence was reached, cells were transfected with the Fugene 6 transfection reagent (Roche) with 1 μg of control or with mouse *Lect2* expression plasmid DNA per well. After 24 h of transfection, the medium was replaced with Dulbecco's modified Eagle's medium (DMEM) containing 10% FBS. When the cells reached to 100% confluence 24 h later, the cells were differentiated into myotubes with DMEM containing 2% horse serum for 24–48 h. Then the cells were stimulated with 100 ng/mL human recombinant insulin for 15 min.

Small Interfering RNA Transfection in C2C12 Myoblasts

C2C12 myoblasts were transiently transfected with a total of 15 nmol/L of small interfering RNA (siRNA) duplex oligonucleotides using Lipofectamine RNAiMAX (Invitrogen), using the reverse-transfection method according to the manufacturer's instructions. A JNK1-specific siRNA with the following sequence was synthesized by Thermo Scientific: 5′-GGAAAGAACUGAUAUACAA-3′ (sense). A JNK2-specific siRNA with the following sequence was synthesized by Thermo Scientific: 5′-GGAAAGAGCUAAUUU ACAA-3′ (sense). Negative control siRNA was purchased from Thermo Scientific. Two days after transfection, cells were pretreated with LECT2 protein then stimulated with 100 ng/mL of human recombinant insulin for 15 min.

RNA Isolation, cDNA Synthesis, and Real-Time PCR Analysis

Total RNA was isolated from cells using the GenElute Mammalian Total RNA Miniprep Kit (Sigma Aldrich). Total RNA was isolated from mouse skeletal muscle and heart using RNeasy Fibrous Tissue Mini Kit (Qiagen). Total RNA was isolated from white adipose tissue using the RNeasy Lipid Tissue Mini Kit (Qiagen). RNA concentrations were measured by a NanoDropR ND-1000 spectrophotometer (NanoDrop Technology). cDNA was synthesized from 100 ng of total RNA using a high-capacity cDNA archive kit (Applied Biosystems, Foster City, CA). Real-time PCR analysis was performed by using TaqMan gene expression assays (Applied Biosystems). Primer sets and TaqMan probes were proprietary to Applied Biosystems (Assays-on-Demand gene expression products). To control for variation in the amount of DNA available for PCR, target gene expression in each sample was normalized relative to the expression of an endogenous control (18S ribosomal RNA or glyceraldehyde-3-phosphate dehydrogenase) (TaqMan control reagent kit; Applied Biosystems).

Treatment With Recombinant LECT2 Protein in C2C12 Myotubes

C2C12 myoblasts were grown in 24-well multiplates; after 100% confluence was reached, cells were differentiated into myotubes by culturing in DMEM supplemented with 2% horse serum for 42 h. C2C12 myotubes were serum-starved and incubated in DMEM for 6 h and then treated with LECT2 recombinant protein for various durations in the absence of serum. Following treatment with LECT2 recombinant protein, cells were stimulated with 100 ng/mL human recombinant insulin for 15 min.

Western Blot Studies in C2C12 Myotubes

After the inulin stimulation, the cells were washed in ice-cold PBS, frozen in liquid nitrogen, and lysed at 4°C in 1× RIPA lysis buffer (Upstat Biotechnology) containing a Complete Mini EDTA-free cocktail tablet (Roche Diagnostics) and PhosSTOP phosphatase inhibitor cocktail tablets (Roche Diagnostics). Lysates then were centrifuged to remove insoluble material. Samples were sonicated with a BIORUPTOR (Cosmo Bio, Tokyo, Japan). Whole-cell lysates were then separated by 5–20% SDS-PAGE gels and were transferred to polyvinylidene fluoride membranes, using an iBlot gel transfer system (Invitrogen). Membranes were blocked in a buffer containing 50 mmol/L Tris, 150 mmol/L NaCl, 0.1% Tween 20, and 5% nonfat milk (pH 7.5) or 5% PhosphoBLOCKER reagent (Cell Biolabs, Inc.) for 1 h at 24°C. They then were probed with antibodies for 16 h at 4°C. Afterward, membranes were washed in a buffer containing 50 mmol/L Tris, 150 mmol/L NaCl, and 0.1% Tween 20 (pH 7.5) and then incubated with anti-rabbit IgG horseradish peroxidase–linked antibody (Cell Signaling) for 1 h at 24°C. Protein signals were detected using ECL Prime Western blotting detection reagent (GE Healthcare UK Ltd.). Densitometric analysis of blotted membranes was performed using ImageJ software (National Institutes of Health; http://rsbweb.nih.gov/ij/).

Glucose or Insulin Tolerance Tests in Mice

In preparation for glucose tolerance testing, mice were fasted for 12 h. After fasting, glucose was administered intraperitoneally, and blood glucose levels were measured at 0, 30, 60, 90, and 120 min. For insulin tolerance testing, mice were fasted for 4 h. After fasting, insulin was administered intraperitoneally, and blood glucose levels were measured. Blood glucose levels were determined by the glucose-oxidase method using Glucocard (Aventis Pharma, Tokyo, Japan). The measurable levels of blood glucose by Glucocard range from 20 to 600 mg/dL. Because mice fed an HFD are much more resistant to insulin than mice fed a standard diet, lower doses of glucose were injected in mice fed an HFD during glucose tolerance testing, as indicated in the legends of Figs. 3 and 4, to avoid the elevation of blood glucose levels to >600 mg/dL. In addition, more doses of insulin were injected to mice fed an HFD during insulin tolerance testing, as indicated in the legends of Figs. 3 and 4, to sufficiently decrease blood glucose levels.

Western Blot Studies in Mice

After 12 h fasting, mice were anesthetized by intraperitoneal administration of sodium pentobarbital. Then insulin (1 units/kg body weight) or PBS (vehicle) was injected through the vena cava. After 10 min, hind-limb muscle tissue, liver tissue, and epididymal white adipose tissue were removed and immediately frozen in liquid

nitrogen. Tissue samples were homogenized using a Polytron homogenizer running at half-maximal speed (15,000 rpm) for 1 min on ice in 1 mL of 1× radioimmunoprecipitation assay lysis buffer (Upstat Biotechnology) containing a Complete Mini EDTA-free cocktail tablet (Roche Diagnostics) and PhosSTOP phosphatase inhibitor cocktail tablets (Roche Diagnostics). Tissue lysates were solubilized by continuous stirring for 1 h at 4°C and centrifuged for 15 min at 14,000 rpm. Protein samples were separated by 5–20% SDS-PAGE gels and were transferred to polyvinylidene fluoride membranes. Serine and tyrosine phosphorylation of specific target proteins was analyzed by Western blotting.

Hyperinsulinemic-Euglycemic Clamp Studies in Mice

Clamp studies were performed as described previously (12,30), with slight modifications. Briefly, 2 days before the study, 13-week-old male C57BL/6J wild-type and *Lect2*-deficient mice were anesthetized using sodium pentobarbital, and an infusion catheter was inserted into the right jugular vein. Before insulin infusion, mice were fasted for 6 h. Clamp studies were performed on conscious and unrestrained animals. Insulin (Novolin R; Novo Nordisk, Denmark) was continuously infused at a rate of 5.0 mU/kg/min, and the blood glucose concentration (monitored every 5 min) was maintained at 100 mg/dL through the administration of glucose (50%, enriched to approximately 20% with [6,6-$^2H_2$]glucose; Sigma) for 120 min. Blood was sampled through tail-tip bleeds at 0, 90, 105, and 120 min for the purpose of determining the rate of glucose disappearance (Rd). Rd values were calculated according to non-steady-state equations, and endogenous glucose production was calculated as the difference between the Rd and the exogenous glucose infusion rates (30).

Exercise Tolerance Test in Mice

Ten-week-old male C57BL/6J wild-type and *Lect2*-deficient mice were set in a running machine. After 5 min of warming up by running and 5 min of rest, mice started running at 11.2 m/min on a 0% incline. Running speed was increased every 5 min until the mice reached exhaustion, defined as when the mouse stopped running for 10 s on the electric tubes.

Acute Exercise Experiment in Mice

Eight-week-old male C57BL/6J mice were randomly divided into two groups: an exercise group and a rest group. All the mice in each group were warmed up for 10 min at 12.6 m/min on a 5% incline. After fasting for 3 h, blood was sampled through tail-tip bleeds. Mice in the exercise group were set in a running machine and started running at 12.6 m/min on a 5% incline. Mice were allowed to have a 5-min rest for every 30 min running. Meanwhile, the mice in the rest group were continually fasted. After 3 h running or resting, blood was sampled again through tail-tip bleeds. Then the mice were anesthetized and killed to isolate the liver tissue.

Starvation Experiment in Mice

Twenty-week-old female C57BL/6J wild-type and *Lect2*-deficient mice were starved for a total of 60 h; water was supplied. Body weight was measured and blood was sampled through tail-tip bleeds 12, 24, and 36 h after starvation; 60 h later, mice were intraperitoneally injected with insulin at a concentration of 10 units/kg body weight. Fifteen minutes later, mice were anesthetized and killed to isolate femoral muscle.

Blood Samples Assays in Mice

Serum levels of *Lect2* were measured using the Ab-Match ASSEMBLY Mouse LECT2 kit (MBL). Serum levels of insulin were determined using a mouse insulin ELISA kit (Morinaga Institute of Biological Science, Inc., Yokohama, Japan), according to the manufacturers' instructions.

Adenovirus-Mediated Gene Transfer in H4IIEC Hepatocytes

H4IIEC hepatocytes were grown to 90% confluence in 24-well multiplates. Cells were infected with adenoviruses encoding dominant-negative (DN) α1 and α2 AMPK, constitutively active (CA) AMPK, or LacZ for 4 h (8.9×106 plaque-forming units/well) (31). We simultaneously expressed α1 and α2 DN AMPK to maximize the effect on AMPK activity. After removing the adenoviruses, the cells were incubated with DMEM for 24 h. Then RNA was isolated from the cells by using GenElute mammalian total RNA miniprep kit (Sigma Aldrich).

Indirect Calorimetry

Mice were housed in standard metabolic cages for 24 h. We used an indirect calorimetry system (Oxymax Equal Flow System; Columbus Instruments, Columbus, OH), in conjunction with the computer-assisted data acquisition program Chart5.2 (AD Instruments, Sydney, Australia), to measure and record oxygen consumption and carbon dioxide production at 5-min intervals. Heat generation was calculated per weight (kilocalories per kilogram per hour).

Measurement of Hepatic Triglyceride Content in Mice

Frozen liver tissue was homogenized in 2 mL ice-cold isopropanol after weighing. After incubation for 10 min with shaking at room temperature, the samples were centrifuged at 3,000 rpm for 10 min, and 1 mL of supernatant was transferred. Triglyceride content in each sample was measured using the commercial Triglyceride E-test WAKO kit (Wako Pure Chemical Industries, Osaka, Japan). Results were normalized to the weight of each liver sample.

Statistical Analyses

All data were analyzed using the Japanese Windows Edition of SPSS version 21.0. Numeric values are reported as the mean ± SEM. Differences between the two groups were assessed using unpaired two-tailed *t* tests. Data involving more than two groups were assessed by ANOVA. Glucose and insulin tolerance tests were examined using repeated-measures ANOVA.

RESULTS

Identification of a Hepatic Secretory Protein Involved in Obesity

To identify hepatokines involved in the pathophysiology of obesity, we performed liver biopsies in humans and conducted a comprehensive analysis of gene expression profiles, as we previously described (12,19,32,33). We obtained ultrasonography-guided percutaneous needle liver biopsies from 10 people with type 2 diabetes and 7 normal subjects. We subjected the biopsies to DNA chip analysis to identify genes whose hepatic expression was significantly correlated with BMI (Supplementary Table 1). As a result, we found a positive correlation between hepatic *Lect2* mRNA levels and BMI, indicating that elevated hepatic *Lect2* mRNA levels are associated with obesity.

Circulating LECT2 Levels Correlate With Adiposity and Insulin Resistance in Humans

To characterize the role of LECT2 in humans, using enzyme-linked immunosorbent assays we measured serum LECT2 levels in participants who visited the hospital for a complete physical examination (26,27) (Supplementary Table 2). We found a significant positive correlation between serum LECT2 levels and BMI and waist circumference (Fig. 1*A* and *B*). LECT2 levels also showed a significant positive correlation with the HOMA-IR and a negative correlation with insulin sensitivity indices (Matsuda index) (Fig. 1*C* and *D*). In addition, serum levels of LECT2 positively correlated with those of SeP, an hepatokine that has already been reported to induce insulin resistance (12) (Fig. 1*E*). Moreover, LECT2 showed a correlation with levels of both HbA_{1c} and systolic blood pressure (Fig. 1*F* and *G*), both of which were reported to be associated with insulin resistance (34,35). These results indicate that serum levels of LECT2 are positively associated with both adiposity and the severity of insulin resistance in humans.

AMPK Negatively Regulates *Lect2* Expression in Hepatocytes

To confirm the elevation of LECT2 in animal models with obesity, we fed C57BL/6J mice an HFD for 8 weeks (Fig. 2*A–F*). An HFD increased body weight in a time-dependent manner (Fig. 2*A*) and tended to increase triglyceride content in the liver (Fig. 2*B*). Hematoxylin and eosin staining showed mild steatosis in the mice fed an HFD (Fig. 2*C*). The expression of *Lect2* was elevated in the livers of the mice fed an HFD, in accordance with steatosis-associated genes such as *Fasn* and *Srebp1c* (Fig. 2*D*). Serum levels of LECT2 showed a sustained increase since a week after beginning the HFD (Fig. 2*E*). In addition, we confirmed that an HFD, even for only a week, resulted in an increase of serum levels of insulin and a decrease of insulin-stimulated Akt phosphorylation in the skeletal muscle of C57BL/6J mice (Supplementary Fig. 1). Importantly, the livers from mice fed an HFD for 8 weeks showed decreased phosphorylation of AMPK (Fig. 2*F*), the energy depletion–sensing kinase that phosphorylates a variety of energy-associated enzymes and functions as a metabolic regulator that promotes insulin sensitivity (36). Since eating an HFD for a short period increased LECT2 concentrations, we then examined the effects of feeding on blood LECT2 levels. LECT2 levels were elevated in blood obtained from fed C57BL/6J mice compared with samples from the fasting mice (Fig. 2*G*). Moreover, AMPK phosphorylation decreased in the livers of the mice that had been fed (Fig. 2*H*). Since *Lect2* expression was inversely correlated with AMPK phosphorylation in the liver, we hypothesized that AMPK negatively regulates LECT2 production in hepatocytes. Exercise is reported to increase phosphorylation and activity of AMPK not only in the skeletal muscle but also in the liver in relation to the intrahepatic elevation of AMP levels (37,38). Thus we examined the actions of aerobic exercise on *Lect2* expression in the liver. C57BL/6J mice were loaded onto a running treadmill for a total of 3 h. Exercise decreased levels of *Lect2* expression and LECT2 protein in the liver (Fig. 2*I* and *J*). Aerobic exercise for 3 h, but not resting, significantly reduced serum levels of LECT2 (Fig. 2*K*). Percentage changes from baseline showed that the reduction of serum LECT2 in the exercise group was significantly larger than that in the rest group (Fig. 2*K*). In addition, aerobic exercise increased AMPK phosphorylation in the liver (Fig. 2*L*). To determine whether AMPK suppresses *Lect2* expression, we transfected H4IIEC hepatocytes with adenoviruses encoding either CA or DN AMPK. First, we found that transfection with CA AMPK significantly decreased mRNA levels of *Lect2* in H4IIEC hepatocytes, similar to those of *G6Pc* that encode the key gluconeogenic enzyme glucose-6 phosphatase that is already known to be suppressed by AMPK (39) (Fig. 2*M*). In contrast, transfection with DN AMPK increased *Lect2* expression (Fig. 2*N*). These results indicate that AMPK negatively regulates LECT2 production in hepatocytes.

Lect2 Deletion Increases Muscle Insulin Sensitivity in Mice

Next we examined the role of LECT2 in the development of insulin resistance in mice. We found that expression of *Lect2* in the liver was overwhelmingly dominant compared with that in other tissues in mice (Fig. 3*A*). This result suggests that the contribution of the other tissues (except the liver) on the circulating levels of LECT2 is very small or negligible in mice. Hence we used systemic knockout mice of LECT2 in the following experiments, although the animal models of liver-specific downregulation for *Lect2* might be more suitable. We confirmed that serum LECT2 was undetectable in *Lect2*-deficient mice by using ELISA (Fig. 3*B*). Body weight, food intake, and heat production at rest were unaffected by *Lect2* knockout (Fig. 3*C–E*). However, the treadmill running challenge revealed that muscle endurance, as assessed by physical exercise, was significantly higher in $Lect2^{-/-}$ mice (Fig. 3*F* and *G*). A glucose or insulin loading test revealed that $Lect2^{-/-}$ mice showed lower blood glucose levels after glucose or insulin injection (Fig. 3*H* and *I*). $Lect2^{-/-}$ mice exhibited an

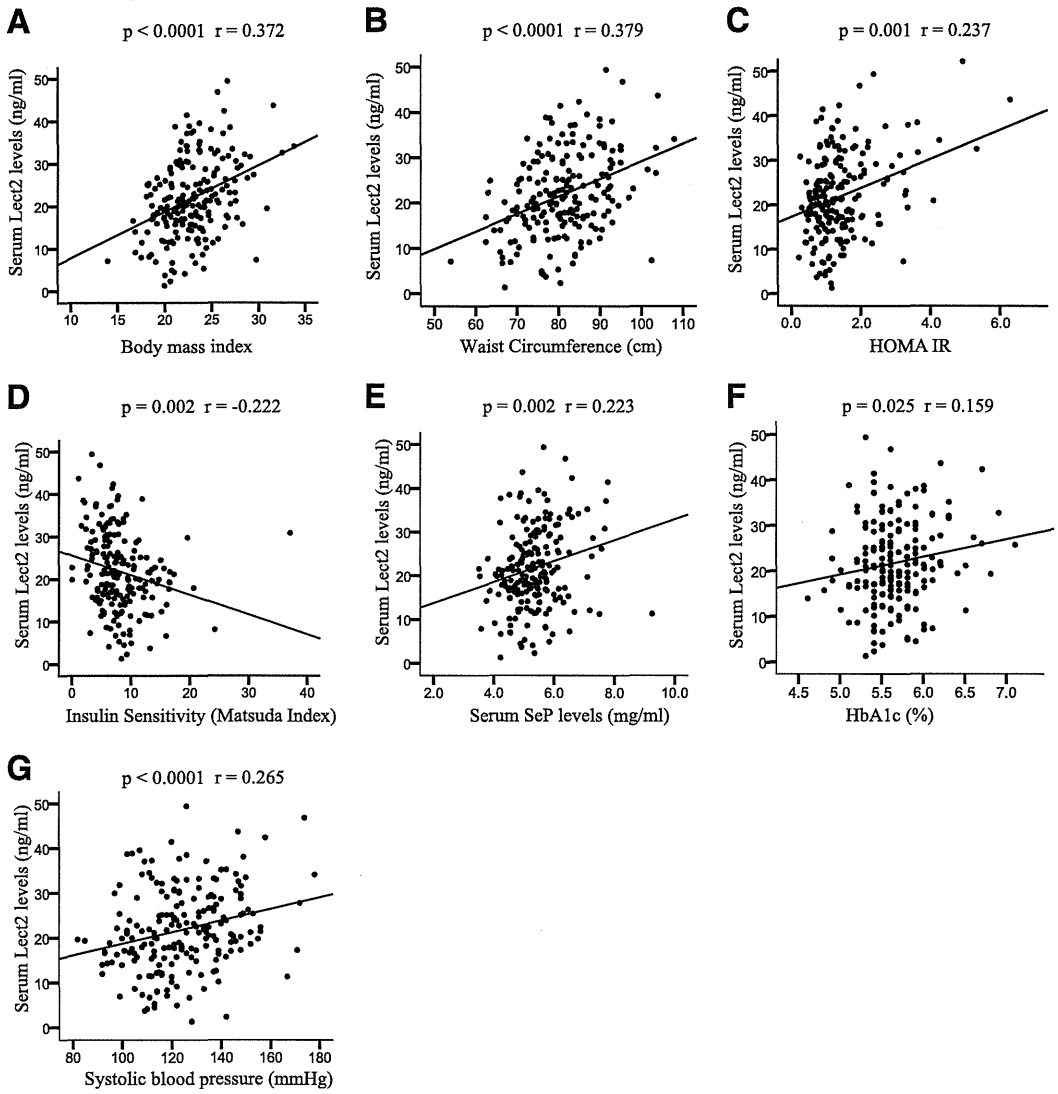

Figure 1—Circulating LECT2 correlates with adiposity and insulin resistance. Graphs show individual correlations between serum levels of LECT2 and BMI (*A*), waist circumference (*B*), HOMA-IR index (*C*), insulin sensitivity (Matsuda index) (*D*), selenoprotein P (SeP) (*E*), HbA_{1c} (*F*), and systolic blood pressure (*G*) in humans (n = 200).

increase in insulin-stimulated Akt phosphorylation in skeletal muscle (Fig. 3*J* and *K*) but not in the liver or adipose tissue (Supplementary Fig. 2*A* and *B*). Furthermore, JNK phosphorylation was unchanged in the liver and adipose tissue of these knockout mice (Supplementary Fig. 2*C* and *D*). Consistent with the results of insulin signaling, hyperinsulinemic-euglycemic clamp studies showed that the glucose infusion rate and peripheral glucose disposal were increased, whereas endogenous glucose production was unaffected by *Lect2* deletion (Fig. 3*L* and Supplementary Fig. 3). In addition, expression of the genes involved in mitochondria and myogenesis, such as *UCP3*, *Myh1*, *Myh2*, and *Ppard*, were upregulated in the muscle of $Lect2^{-/-}$ mice (Fig. 3*M*). These results indicate that deletion of *Lect2* increases insulin sensitivity in skeletal muscle in mice.

Lect2 Deletion Attenuates Muscle Insulin Resistance in Dietary Obese Mice

To elucidate further the role of LECT2 in the development of obesity-associated insulin resistance, we fed *Lect2*-deficient mice an HFD. HFD-induced body weight gain was smaller in *Lect2*-deficient mice compared with wild-type animals (Fig. 4*A*). To examine the mechanism by which *Lect2*-deficient mice were less obese after eating an HFD, we measured food intake and heat production in *Lect2*-deficient mice fed an HFD for only a week, when the body

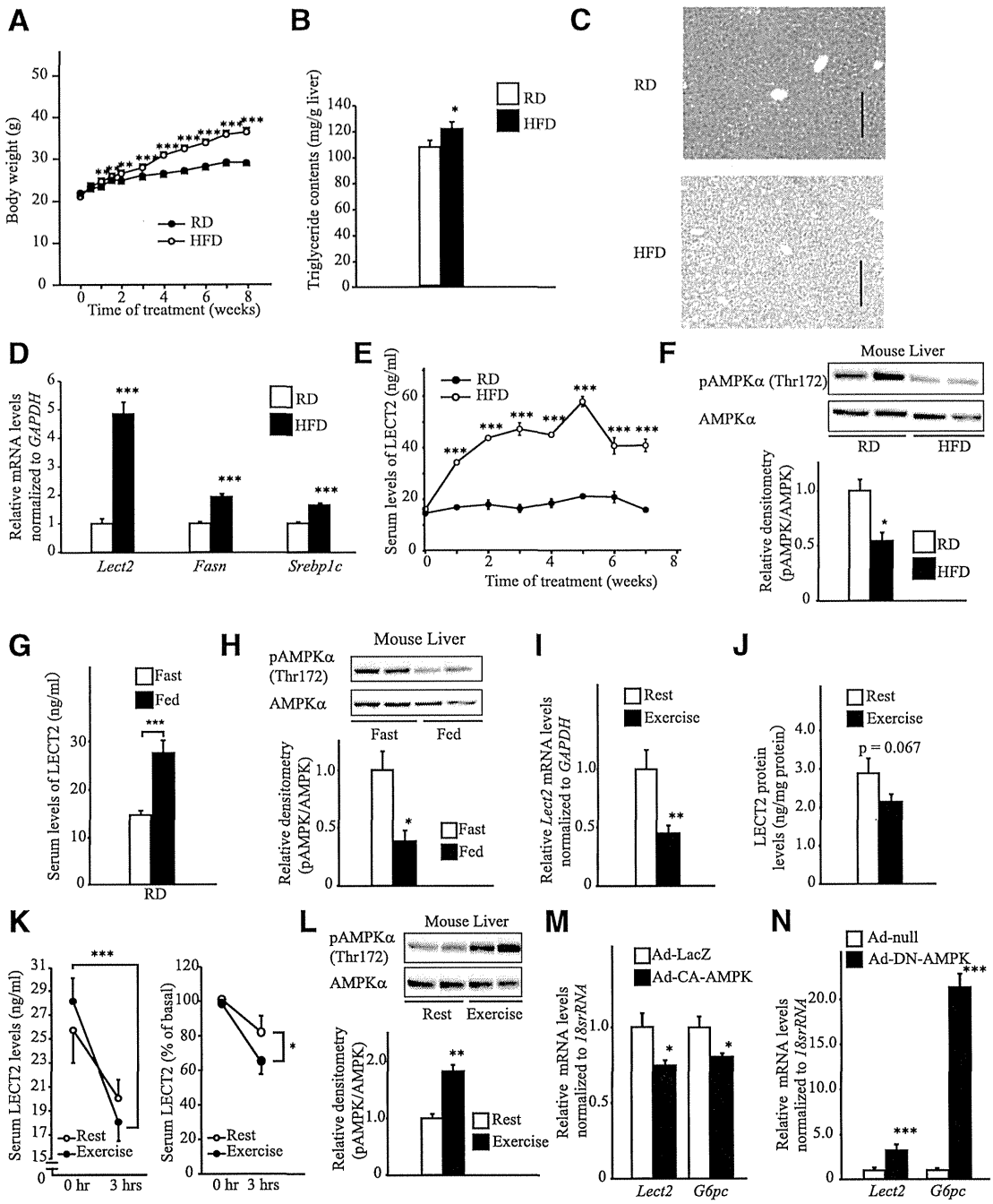

Figure 2—AMPK negatively regulates *Lect2* expression in the liver. *A*: Body weight of C57BL/6J mice fed an HFD (n = 15) or regular diet (RD; n = 16). Five-week-old male mice were fed an HFD for 8 weeks. *B*: Triglyceride contents in the livers of C57BL/6J mice fed an HFD or an RD for 8 weeks (n = 7 or 8). *C*: Hematoxylin and eosin staining of livers from C57BL/6J mice fed an HFD or an RD for 8 weeks. *D*: mRNA levels for *Lect2*, *Fasn*, and *Srebp1c* in the livers of C57BL/6J mice fed an HFD or an RD for 8 weeks (n = 7 or 8). *E*: Changes of blood levels of LECT2 in C57BL/6J mice fed an HFD (n = 8) or an RD (n = 8). Blood samples were obtained after fasting for 12 h. *F*: Phosphorylation of AMPK in the livers of C57BL/6J mice fed an HFD or an RD after a 12-h fast (n = 4). *G*: Blood levels of LECT2 from C57BL/6J mice following fasting for 12 h and subsequent feeding for 12 h (n = 7 or 8). *H*: Phosphorylation of AMPK in the livers of C57BL/6J mice following fasting for 12 h and subsequent feeding for 12 h (n = 3). *I*: Levels of *Lect2* mRNA in the livers of C57BL/6J mice following running exercise for 3 h (n = 7–8). *J*: Protein levels of LECT2 in the livers of C57BL/6J mice following running exercise for 3 h (n = 7–8). *K, left*: Serum levels of LECT2 in C57BL/6J mice before and after running exercise for 3 h (n = 8; paired t test). *K, right*: Percentage changes of serum LECT2 after running exercise for 3 h (unpaired t test). *L*: Phosphorylation of AMPK in the livers of C57BL/6J mice following running exercise for 3 h (n = 3 or 4). *M*: Effects of CA AMPK on mRNA levels of *Lect2* and *G6pc* in H4IIEC hepatocytes (n = 4). *N*: Effects of dominant-negative (DN) AMPK on

weight was comparable between the wild-type and knockout mice (Supplementary Fig. 4*A*). Food intake was unaffected (Supplementary Fig. 4*B*), but heat production as measured by oxygen consumption was significantly increased in *Lect2*-deficient mice fed an HFD (Supplementary Fig. 4*C*) in both light and dark phases (Supplementary Fig. 4*D* and *E*). Eleven weeks later after eating an HDF, serum levels of insulin and blood levels of glucose decreased in these knockout mice (Fig. 4*B* and *C*). A glucose or insulin loading test revealed that *Lect2* knockout mice showed lower blood glucose levels after glucose or insulin injection (Fig. 4*D* and *E*). Consistent with the result of the insulin loading test, Western blotting revealed that insulin-stimulated Akt phosphorylation increased in the skeletal muscle of these knockout animals (Fig. 4*F* and *G*). In contrast, JNK phosphorylation significantly decreased in the skeletal muscle of *Lect2*-deficient mice (Fig. 4*H* and *I*). Furthermore, we examined muscle insulin signaling in *Lect2*-deficient mice fed an HFD for only 2 weeks, when the body weight was comparable between the wild-type and knockout mice (Supplementary Fig. 5*A–C*). Insulin-stimulated Akt phosphorylation was significantly increased in the muscle of *Lect2*-deficient mice under conditions of an HFD for 2 weeks (Supplementary Fig. 5*D* and *E*). These results indicate that *Lect2* deletion reduces muscle insulin resistance in dietary obese mice.

Starvation Abolishes the Insulin-Sensitive Phenotype in *Lect2*-Deficient Mice

Next, to elucidate the role of LECT2 in a condition of severe undernutrition, we starved *Lect2*-deficient mice for 60 h. Starvation decreased body weight and blood glucose levels in a time-dependent manner, whereas there was no significance between wild-type and *Lect2*-deficient mice (Fig. 5*A* and *B*). Consistent with the changes of body weight, serum levels of LECT2 in wild-type animals significantly decreased during the period of starvation (Fig. 5*C*). Before starvation, serum levels of insulin in *Lect2* knockout mice were lower compared with wild-type mice (Fig. 5*D*). However, the starvation reduced insulin levels to the extent to which the difference abolished between the two groups (Fig. 5*D*). Insulin-stimulated Akt phosphorylation in skeletal muscle also showed no difference between the two groups after 60 h of starvation (Fig. 5*E*). These results indicate that starvation abolishes the insulin-sensitive phenotype in *Lect2*-deficient mice.

LECT2 Impairs Insulin Signaling by Activating JNK in C2C12 Myotubes

First, to examine the effect of LECT2 on insulin signaling in vitro, we transfected C2C12 myocytes with a plasmid expression vector encoding mouse LECT2. Expression of endogenous *Lect2* was negligible in C2C12 myocytes transfected with a negative control vector (Fig. 6*A* and *B*). We confirmed that C2C12 myotubes transfected with the *Lect2* expression vector expressed *Lect2* mRNA and released LECT2 protein into the culture medium (Fig. 6*A* and *B*). LECT2 transfection suppressed myotube differentiation in C2C12 cells (Fig. 6*C*). The cells transfected with the *Lect2* vector showed a decrease in insulin-stimulated Akt phosphorylation (Fig. 6*D*) and an increase in basal JNK phosphorylation (Fig. 6*E*).

To further confirm the acute action of LECT2 on insulin signaling, we treated C2C12 myotubes with recombinant LECT2 protein at nearly physiological concentrations. Treatment with 400 ng/mL of LECT2 protein for 3 h decreased insulin-stimulated Akt phosphorylation (Fig. 6*F*). In addition, treatment with LECT2 protein for 30–60 min transiently increased JNK phosphorylation in C2C12 myotubes (Fig. 6*G*). LECT2-induced JNK phosphorylation occurred in a concentration-dependent manner (Fig. 6*H*). To determine whether the JNK pathway mediates LECT2-induced insulin resistance, we transfected C2C12 myoblasts with siRNAs specific for JNK1 and JNK2. Because knockdown of JNK is known to alter the myotube differentiation in C2C12 myotubes (40), we used undifferentiated C2C12 myoblasts to purely assess the action of LECT2 on insulin signal transduction in the following experiments. Double knockdown of JNK1 and JNK2 rescued the cells from the inhibitory effects of LECT2 on insulin signaling (Fig. 6*I*). Inflammatory signals and endoplasmic reticulum stress are known to be powerful inducers of JNK (41). However, the markers of neither inflammation nor endoplasmic reticulum stress were changed in C2C12 myotubes overexpressed with *Lect2* and in the skeletal muscle of *Lect2* knockout mice (Supplementary Fig. 4). These in vitro experiments indicate that, at nearly physiological concentrations, LECT2 impairs insulin signal transduction by activating JNK in C2C12 myocytes.

DISCUSSION

Our research reveals that the overproduction of the hepatokine LECT2 contributes to the development of muscle insulin resistance in obesity (Fig. 7). Recent growing evidence suggests a central role for fatty liver disease in the development of insulin resistance in obesity (4,42). Kotronen et al. (43) have reported that intrahepatocellular rather than intramyocellular fat is associated with hyperinsulinemia independent of obesity in nondiabetic men. Fabbrini et al. (44) have revealed that intrahepatic triglyceride, but not visceral adipose tissue, is a better marker of multiorgan insulin resistance associated with obesity. D'Adamo et al. (45) have shown that obese

mRNA levels of *Lect2* and *G6pc* in H4IIEC hepatocytes ($n = 4$). Data in *A* and *B* and *D–N* represent the means ± SEM. $^{*}P < 0.05$, $^{**}P < 0.01$, $^{***}P < 0.001$. *Fasn*, fatty acid synthase; *G6pc*, glucose-6 phosphatase; *Srebp1c*, sterol regulatory-element binding protein-1c.

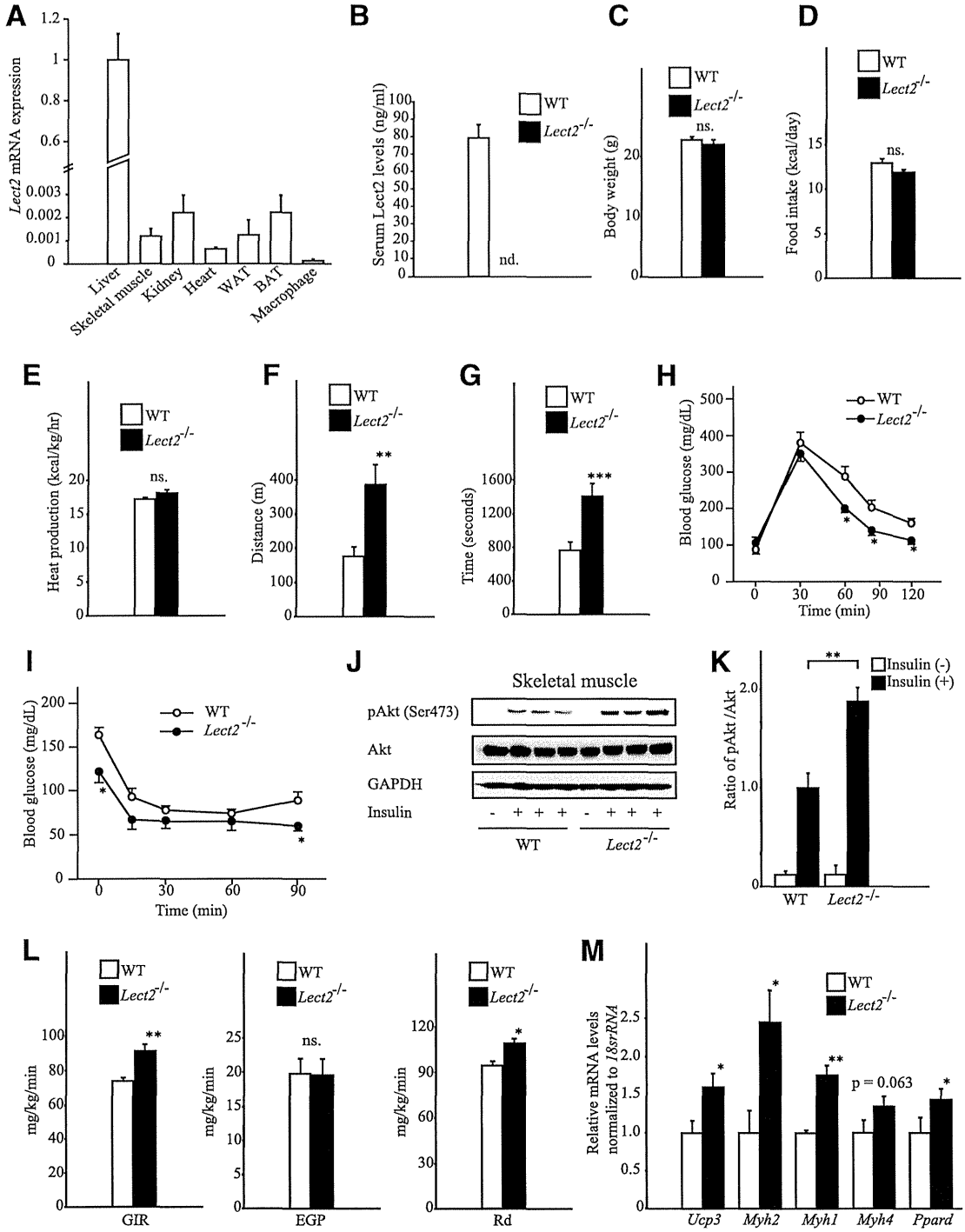

Figure 3—*Lect2* deletion increases muscle insulin sensitivity in mice. *A*: *Lect2* mRNA levels in various tissues of C57BL/6J mice (n = 4–8). *B:* Serum levels of LECT2 in *Lect2*-deficient and wild-type (WT) mice fed an HFD for 10 weeks (n = 9–13). Blood samples were obtained during the fed condition. *C*: Body weight of *Lect2*-deficient and wild-type mice fed a regular diet (n = 6–8). *D*: Food intake of *Lect2*-deficient and wild-type mice (n = 6–8). *E*: Heat production of *Lect2*-deficient and wild-type mice (n = 6–8). *F, G*: Running endurance was tested in *Lect2*-deficient and wild-type mice (n = 7 or 8). Running endurance is depicted as distance (*F*) and time (*G*). Intraperitoneal glucose (*H*) and insulin (*I*) tolerance tests in *Lect2*-deficient and wild-type mice (n = 7 or 8). Glucose and insulin were administered at doses of 2.0 g/kg body weight and 1.0 units/kg body weight, respectively. *J, K*: Western blot analysis and quantification of phosphorylated Akt in skeletal muscle of *Lect2*-deficient and wild-type mice (n = 5). Nineteen-week-old female mice were stimulated with insulin (administered through the vena cava) at doses of 1 unit/kg